

Anisotropic spin splitting and spin relaxation in asymmetric zinc-blende semiconductor quantum structures

J. Kainz* and U. Rössler

Institut für Theoretische Physik, Universität Regensburg, 93040 Regensburg, Germany

R. Winkler

Institut für Technische Physik III, Staudtstr. 7, D-91058 Erlangen, Germany

(Dated: April 29, 2019)

Spin relaxation due to the D'yakonov-Perel' mechanism is intimately related with the spin splitting of the electronic states. We determine the spin relaxation rates from anisotropic spin splittings of electron subbands in n-(001) zinc-blende semiconductor quantum structures calculated self-consistently in the multi-band envelope function approach. The giant anisotropy of spin relaxation rates found for different spin-components in the (001) plane can be ascribed to the interplay between the bulk and quantum well inversion asymmetry. One of the in-plane relaxation rates may exhibit a striking nonmonotonous dependence on the carrier density.

PACS numbers: 72.25.Rb

Keywords: spin relaxation; spin splitting; bulk inversion asymmetry; structural inversion asymmetry

I. INTRODUCTION

The spin degree of freedom of electrons in solids has recently attracted much interest^{1,2,3,4,5} in the perspective of spintronic devices, which require long spin relaxation times. Thus, a quantitative understanding of the dependence of spin-relaxation times on the system parameters is needed for the desired engineering of systems with the required properties as well as for the interpretation of measured values.^{6,7,8,9} It is generally accepted¹⁰ that in bulk zinc-blende type semiconductors and in quantum well (QW) structures based on these materials electronic spin relaxation is governed by the D'yakonov-Perel'^{11,12} (DP) and the Bir-Aronov-Pikus¹³ mechanisms. The former mechanism becomes dominant in n-doped (001)-grown QW systems, which we consider here. The DP mechanism is intimately related with the spin splitting of the electronic subbands caused by the lacking inversion symmetry.¹⁴ It can result from the bulk crystal structure (bulk inversion asymmetry, BIA¹⁵) but also from the QW structure (structural inversion asymmetry, SIA¹⁶). Making use of this relation, Averkiev et al.^{14,17} employ a simple variational calculation for a triangular potential model of n-doped GaAs heterostructures and include BIA and SIA terms as a perturbation to calculate spin-splitting and DP spin-relaxation rates. The simplicity of this approach raises the question of the reliability of these results in view of a more rigorous calculation, as will be presented in this paper.

In this contribution, we determine the electron spin relaxation rates for longitudinal (in growth direction) and transverse (in-plane) spin components in asymmetric n-doped (001)-grown zinc-blende semiconductor quantum structures using the anisotropic spin splitting obtained from self-consistent calculations in the multi-band envelope-function approximation (EFA).¹⁸ We investigate the dependence of these rates on the QW width and carrier concentration for the material systems Al-

GaAs/GaAs and AlGaSb/InAs, and compare our results for the former system with those of Ref. 14.

II. DP MECHANISM AND SPIN SPLITTING

The DP spin relaxation is described in a single band approach by considering the time evolution of the electron spin-density vector

$$S = \langle \text{tr}(\rho_{\mathbf{k}} \boldsymbol{\sigma}) \rangle = \sum_{\mathbf{k}} \text{tr}(\rho_{\mathbf{k}} \boldsymbol{\sigma}), \quad (1)$$

where \mathbf{k} is the electron wave vector, $\boldsymbol{\sigma}$ the vector of Pauli spin matrices, and $\rho_{\mathbf{k}}$ the 2×2 electron spin-density matrix. The dynamics of $\rho_{\mathbf{k}}$ is ruled by a Bloch equation containing the spin-orbit coupling $H_{\text{so}} = \hbar \boldsymbol{\sigma} \cdot \boldsymbol{\Omega}(\mathbf{k})$ and the (spin independent) momentum scattering, e.g., with phonons and (nonmagnetic) impurities characterized by a momentum scattering time τ_p . The spin-orbit coupling is analogous to a Zeeman term, but with an effective magnetic field $\boldsymbol{\Omega}(\mathbf{k})$ that depends on the underlying material and geometry and on the electron wave vector \mathbf{k} . The vector $\text{tr}(\rho_{\mathbf{k}} \boldsymbol{\sigma})$ precesses about $\boldsymbol{\Omega}(\mathbf{k})$ which eventually results in spin relaxation. However, momentum scattering changes \mathbf{k} and thus the direction and magnitude of $\boldsymbol{\Omega}(\mathbf{k})$ felt by the electrons. Therefore, frequent scattering (on the time scale of $|\boldsymbol{\Omega}(\mathbf{k})|^{-1}$) suppresses the precession and consequently the spin relaxation. This is the motional-narrowing behavior that is typical for the DP mechanism, according to which the spin relaxation rate $\tau_s^{-1} \propto \tau_p$.¹²

Due to time reversal invariance we have $\boldsymbol{\Omega}(0) = 0$. At finite \mathbf{k} the spin-orbit coupling H_{so} causes a spin splitting $2\hbar|\boldsymbol{\Omega}(\mathbf{k})|$ of the subband structure. It exists already in bulk semiconductors with broken inversion symmetry. In this article we focus on semiconductors with a zinc-blende structure where the BIA spin splitting of the electron

states is characterized in leading order by the Dresselhaus or k^3 term^{15,19}

$$\Omega_{\text{BIA}}(\mathbf{k}) = \frac{\gamma}{\hbar} \begin{pmatrix} k_x (k_y^2 - k_z^2) \\ k_y (k_z^2 - k_x^2) \\ k_z (k_x^2 - k_y^2) \end{pmatrix} \quad (2)$$

where γ is a material dependent parameter. In the following we will assume that the z axis is perpendicular to the QW plane. In asymmetric QW's SIA gives rise to a second contribution to spin-orbit coupling. Its leading term, linear in $\mathbf{k}_{\parallel} = (k_x, k_y, 0)$ is frequently called the Rashba term.¹⁶ It is characterized by the effective field

$$\Omega_{\text{SIA}}(\mathbf{k}_{\parallel}) = \frac{\alpha}{\hbar} \begin{pmatrix} k_y \\ -k_x \\ 0 \end{pmatrix} \quad (3)$$

with a prefactor α that depends on the material parameters of the underlying semiconductor bulk material (like γ) but in addition also on the asymmetry of the QW in growth direction. In first order perturbation theory for (001) oriented QW's the terms k_z (and powers thereof) in the BIA term are replaced by expectation values with respect to the subband function, thus one has²⁰

$$\Omega(\mathbf{k}_{\parallel}) = \frac{\gamma}{\hbar} \begin{pmatrix} k_x (k_y^2 - \langle k_z^2 \rangle) \\ k_y (\langle k_z^2 \rangle - k_x^2) \\ 0 \end{pmatrix} + \Omega_{\text{SIA}}(\mathbf{k}_{\parallel}). \quad (4)$$

Within the DP mechanism the relaxation of the components of \mathbf{S} are ruled by¹²

$$\frac{\partial}{\partial t} S_i = -\frac{1}{\tau_i} S_i \quad (5)$$

with $i = z, +, -$ corresponding to the components of \mathbf{S} along [001], [110], and $\bar{[1}10]$, $S_{\pm} = 1/\sqrt{2}(S_x \pm S_y)$, and spin-relaxation rates¹⁴

$$\frac{1}{\tau_z} = \frac{4\tau_p}{\hbar^2} \left[(\gamma^2 \langle k_z^2 \rangle^2 + \alpha^2) k_F^2 - \frac{\gamma^2 \langle k_z^2 \rangle k_F^4}{2} + \frac{\gamma^2 k_F^6}{8} \right] \quad (6a)$$

$$\frac{1}{\tau_{\pm}} = \frac{2\tau_p}{\hbar^2} \left[k_F^2 (\pm\alpha - \gamma \langle k_z^2 \rangle) \left(\pm\alpha - \gamma \langle k_z^2 \rangle + \frac{\gamma}{2} k_F^2 \right) + \frac{\gamma^2 k_F^6}{8} \right]. \quad (6b)$$

Here we have assumed an isotropic momentum scattering and a degenerate electron system. The rates (6) depend explicitly on the carrier density n via the radius k_F of the Fermi circle and implicitly via the self-consistent subband functions in the expectation values of k_z^2 .

In a previous evaluation of Eq. (6) in n-doped (001) grown GaAs heterostructures, Averkiev et al.¹⁴ employed the triangular potential model and the variational subband function of Ref. 21, thus assuming an infinite barrier

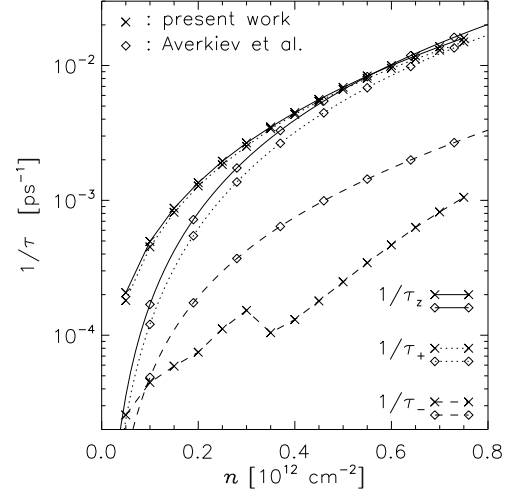


FIG. 1: Comparison of data from Ref. 14 with present results (marked “+”) for the spin relaxation rates τ_z^{-1} , τ_+^{-1} , τ_-^{-1} as a function of charge density n for an asymmetrically doped AlAs/GaAs heterostructure. The range of n is chosen so that only the lowest (spin-split) subband is occupied.

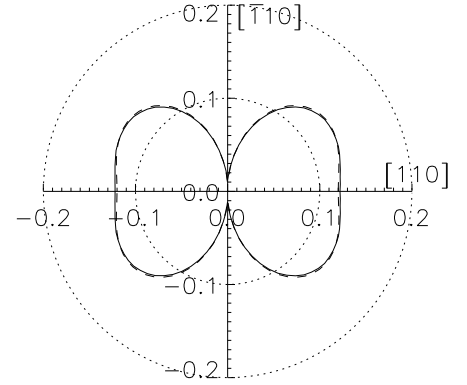


FIG. 2: Polar plot of the calculated (full line) and fitted (dashed line) spin splitting $2\hbar|\Omega(\mathbf{k}_{\parallel})|$ in meV for \mathbf{k}_{\parallel} at the Fermi contour in an asymmetrically doped (001) AlAs/GaAs heterostructure with charge density $n = 3 \times 10^{11} \text{ cm}^{-2}$.

at the interface and working in the single-band approximation. In their model, the electric field varies linearly with the carrier density n , which results in $\alpha \propto n$. Using Eq. (6) and a tabulated value of $\gamma = 27 \text{ eV}\text{\AA}$ (appropriate for bulk GaAs) these authors calculate the relaxation rates for carrier densities up to $2.5 \times 10^{13} \text{ cm}^{-2}$. (Their results for a smaller range of n are reproduced in Fig. 1.) However, carrier densities in real AlAs/GaAs quantum structures with occupation of the lowest subband only are limited to $n \lesssim 8 \times 10^{11} \text{ cm}^{-2}$ (see Ref. 22 and dis-

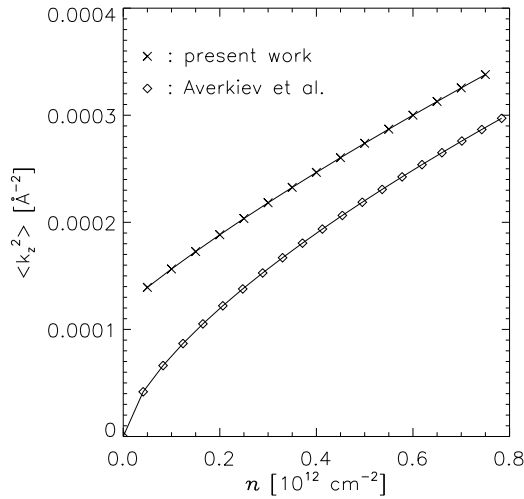


FIG. 3: Comparison of data from Ref. 14 with present results for the expectation value $\langle k_z^2 \rangle$ as a function of charge density n for an asymmetrically doped AlAs/GaAs heterostructure.

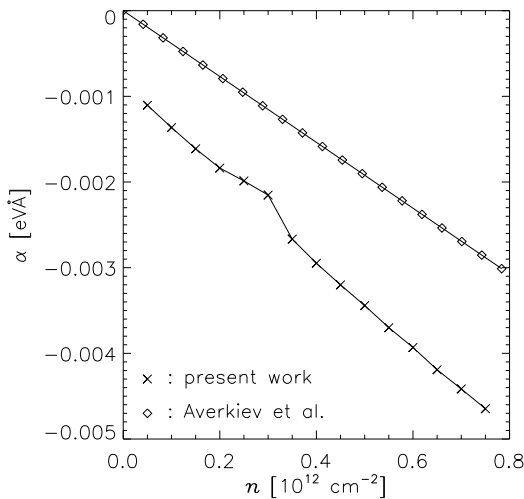


FIG. 4: Comparison of data from Ref. 14 with present results for the Rashba coefficient α as a function of charge density n for an asymmetrically doped AlAs/GaAs heterostructure.

cussion below). Moreover, the approach of Averkiev et al. does not yield full self-consistency nor does it include nonparabolic corrections or effects due to the barrier material, which have to be taken into account for finite barriers.

In order to overcome these deficiencies we perform fully self-consistent calculations of the subband spin splitting in the multiband EFA (considering five levels or 14 bands¹⁸) in application to (001) oriented AlGaAs/GaAs and AlGaSb/InAs QW's, n-doped on one side. Such calculations, which include in a systematic way the BIA nonparabolicity modified by the QW confinement and

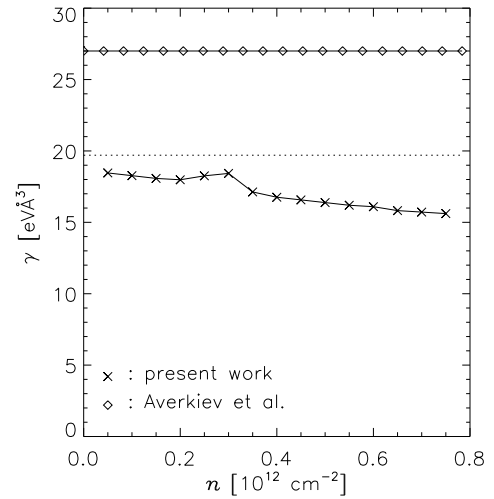


FIG. 5: Comparison of data from Ref. 14 with present results for the BIA coefficient γ as a function of charge density n for an asymmetrically doped AlAs/GaAs heterostructure. The dotted line indicates the value for bulk GaAs.

the SIA or Rashba term, have successfully explained the anisotropic spin splitting measured with inelastic light-scattering.²³ Figure 2 shows a typical polar plot of the calculated spin splitting in the (k_x, k_y) plane (solid contour). The striking feature is the pronounced anisotropy with the strongly reduced spin splitting in the $[\bar{1}10]$ direction. Before employing Eq. (6) to convert these spin splittings into spin relaxation rates, the parameters α and γ have to be determined such that Eq. (4) reproduces the calculated spin splittings of the multiband EFA calculation. Hereby, the expectation value $\langle k_z^2 \rangle$ (shown in Fig. 3 together with the estimate $\langle k_z^2 \rangle \propto n^{2/3}$ used in Ref. 14) is evaluated using the EFA wave function and $k_F = \sqrt{2\pi n}$. The quality of this approach is demonstrated in Fig. 2 (dashed contour). The parameters α and γ change as a function of n (Figs. 4 and 5). For α this dependence is expected as α contains the expectation value of the electric field. Our more realistic calculation gives the absolute value of the Rashba coefficient substantially larger than that of Ref. 14. The dependence of γ on n (which is only moderate) reflects higher order nonparabolicity corrections with increasing Fermi energy known from the bulk material.²⁴ For our set of band parameters, the bulk values of γ are $19.7 \text{ eV}\text{\AA}^3$ for GaAs³¹ and $18.5 \text{ eV}\text{\AA}^3$ for AlAs.

Recently Lau et al.²⁵ have performed similar calculations, yet for symmetrically doped QW's in order to compare with experimental data obtained from multiple QW's.⁷ Our focus here is on asymmetric single QW's and the interplay between SIA and BIA terms, which require fully self-consistent EFA calculations.

The simpler 8-band model, which takes into account BIA only perturbatively, yields qualitatively the same spin splitting as the 14-band Hamiltonian. However, the

magnitude of the spin splitting is about 10–20% larger in the 8-band model.²³ Therefore, all results given in this paper are based on the more realistic 14-band model.

III. CALCULATED SPIN RELAXATION RATES

In this section we present our results for the spin-relaxation rates obtained from Eq. (6) with the parameters $\langle k_z^2 \rangle$, α and γ determined within the 14-band EFA calculations. This is done by assuming a momentum-scattering time $\tau_p = 0.1$ ps. As all rates are proportional to τ_p they may be readily rescaled. For all calculations presented in this paper the range of n is chosen such that only the lowest (spin-split) subband is occupied. In Fig. 1 our results are shown for a AlAs/GaAs heterostructure in comparison with the data from Ref. 14. (Note that in Ref. 14 τ_+ and τ_- are interchanged³².) Both in Ref. 14 and in our calculation, the rates τ_z^{-1} and τ_+^{-1} increase monotonously with the carrier density and are close to each other over the whole range. For the higher densities ($n \gtrsim 0.4 \times 10^{12} \text{ cm}^{-2}$) our results for τ_z^{-1} and τ_+^{-1} coincide with the respective data from Ref. 14, whereas our relaxation rates are generally much larger for small n . This can be attributed to the fact that in Ref. 14 it was assumed that $\langle k_z^2 \rangle \propto n^{2/3}$, while in our calculations $\langle k_z^2 \rangle$ does not tend towards zero for small n (Fig. 3). Our results for τ_-^{-1} are generally much smaller than those of Ref. 14 and show also a pronounced nonmonotonous behavior around $n \approx 0.4 \times 10^{12} \text{ cm}^{-2}$, which is not present in Ref. 14. A detailed explanation of the origin of this feature will be given below. The small oscillation below and above the dip at $n \approx 0.4 \times 10^{12} \text{ cm}^{-2}$ is numerical noise.

Spin relaxation rates calculated as a function of the QW width L and carrier density n are shown in Fig. 6 for single-side n-doped QW's with (001) orientation for the material systems Al_{0.35}Ga_{0.65}As/GaAs and Al_{0.3}Ga_{0.70}Sb/InAs. With increasing L the asymmetric single-side doped QW's become more and more similar to a single heterostructure, and therefore the results for $L \gtrsim 200 \text{ \AA}$ are almost the same as for a heterostructure. Similar to the GaAs/AlAs system of Fig. 1 the rates τ_z^{-1} and τ_+^{-1} are close to each other in all cases, while τ_-^{-1} is distinctly smaller (frequently more than an order of magnitude) and shows the nonmonotonous dependence on n . Both the GaAs and the InAs QW's show qualitatively the same behavior.

In Fig. 6 we have a dip in the density dependence of τ_-^{-1} that is most pronounced for the InAs QW's. This feature, not seen in Ref. 14, appears here due to the differences in $\langle k_z^2 \rangle$, α and γ (see Figs. 3,4,5). They cause in our calculations the first term in the expression defining τ_-^{-1} [Eq. (6b)] to become negative in a certain range of n and therefore lead to a nonmonotonous behavior.

The origin of the dip in τ_-^{-1} can be understood more clearly within a simplified picture of the DP mechanism, where we assume that the spin relaxation rate for the

spin component in the direction e is only effected by those components of the effective field $\Omega(\mathbf{k}_\parallel)$ that are perpendicular to e . In analogy with the behavior of spin relaxation rates for nuclear magnetic resonance²⁶ the spin relaxation rate τ_-^{-1} of the spin component in the direction [110] should be proportional to the average of the squared effective field components perpendicular to that direction:

$$\tau_-^{-1} \propto \left(\langle \Omega_{[110]}^2 \rangle(k_F) + \langle \Omega_{[001]}^2 \rangle(k_F) \right), \quad (7)$$

where $\langle \Omega_{[110]}^2 \rangle(k_F)$ represents an average over the Fermi contour

$$\langle \Omega_{[110]}^2 \rangle(k_F) = \frac{1}{2\pi} \int_0^{2\pi} d\varphi \Omega_{[110]}^2(\mathbf{k}_F(\varphi)) \quad (8a)$$

and $\Omega_{[110]}(\mathbf{k}_F(\varphi))$ denotes a projection of $\Omega(\mathbf{k}_F(\varphi))$ on the direction [110]

$$\Omega_{[110]}(\mathbf{k}_F(\varphi)) = \Omega(\mathbf{k}_F(\varphi)) \cdot \begin{pmatrix} 1/\sqrt{2} \\ 1/\sqrt{2} \\ 0 \end{pmatrix}, \quad (8b)$$

$$\mathbf{k}_F(\varphi) = k_F \begin{pmatrix} \cos \varphi \\ \sin \varphi \\ 0 \end{pmatrix}. \quad (8c)$$

As the projection of $\Omega(\mathbf{k}_\parallel)$ onto the [001] direction vanishes, $\langle \Omega_{[001]}^2 \rangle(k_F)$ is equal to zero. Hence, $\langle \Omega_{[110]}^2 \rangle(k_F)$ is a measure of the relaxation rate τ_-^{-1} . We calculated this quantity as a function of n (Fig. 7) and found the same behavior as for τ_-^{-1} , thus confirming our interpretation. In the same line of arguments τ_+^{-1} is essentially determined by $\langle \Omega_{[110]}^2 \rangle(k_F)$ and, in fact, this quantity exhibits a monotonous dependence on n similar to τ_+^{-1} in Figs. 1 and 6.

IV. PROPOSED MEASUREMENTS

Our calculations indicate a large difference of the spin relaxation times for spins oriented in \pm and z direction. This feature is quite universal; it appears both in GaAs- and InAs-based systems over a wide range of well widths and carrier densities. In a certain density range ("dips" in Fig. 6) the spin relaxation times can differ by more than two orders of magnitude. Therefore, we expect that this difference can be observed experimentally.

The creation of spins oriented in z direction using optical orientation techniques and the measurement of their relaxation has already been demonstrated.^{6,7,8,9} For the creation of an in-plane spin orientation a spin-injection technique similar to the paradigmatic spin transistor²⁷ can be used. Here the carrier density can be varied by means of a gate electrode and the spin relaxation can be detected via the source-drain current.

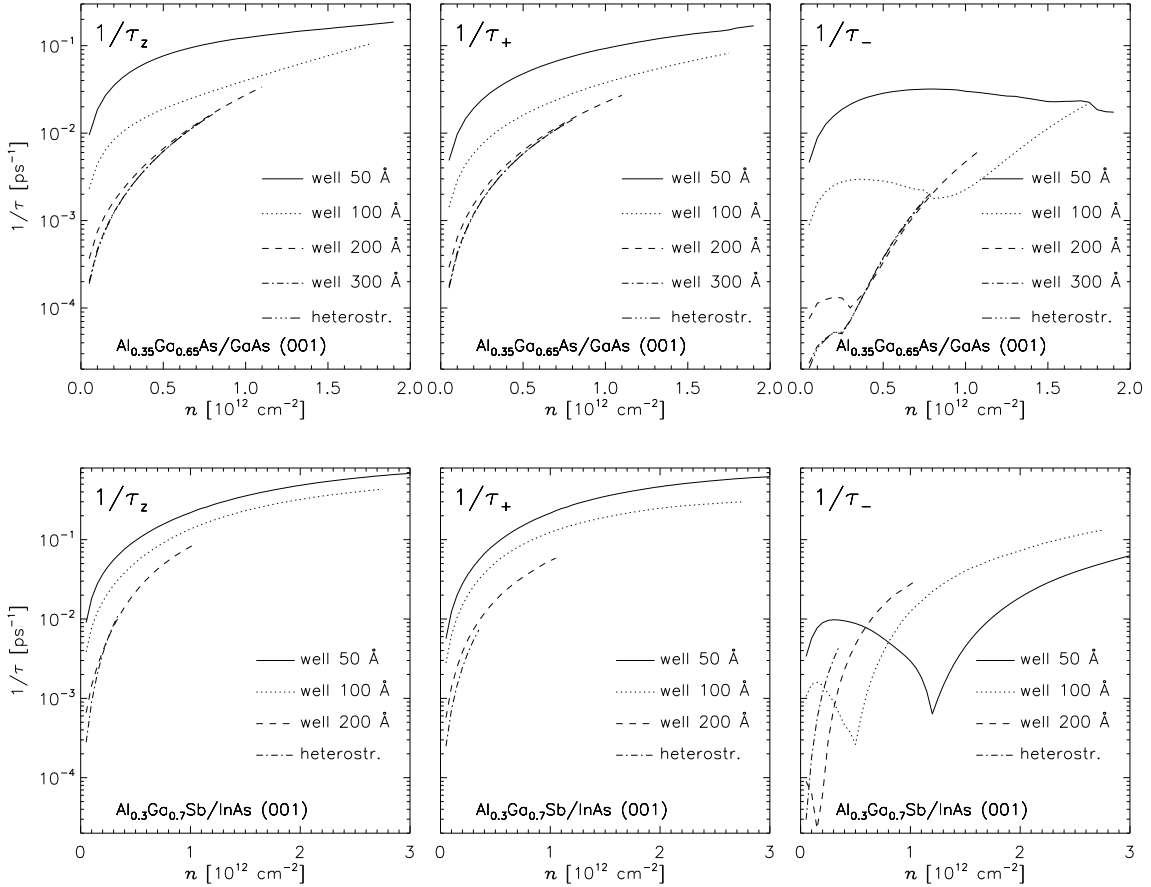


FIG. 6: Spin relaxation rates τ_z^{-1} , τ_+^{-1} , τ_-^{-1} as a function of charge density n for $\text{Al}_{0.35}\text{Ga}_{0.65}\text{As}/\text{GaAs}$ (001) (upper row) and $\text{Al}_{0.3}\text{Ga}_{0.7}\text{Sb}/\text{InAs}$ (001) (lower row) quantum wells with widths $L = 50, 100, 200 \text{ \AA}$ and for a simple heterostructure. The range of n is chosen so that only the lowest (spin split) subband is occupied.

We propose a second scheme for the creation of in-plane excess spins and the measurement of their relaxation time: In a first step, spins oriented in z direction are created with conventional optical orientation techniques. These can be rotated into the plane of the QW by means of a so-called tipping pulse, as demonstrated by Gupta *et al.*²⁸ After a certain delay, the spins are rotated back into the z direction, so that the magnitude of the remaining spin polarization can be measured. By changing the delay time the spin relaxation for an arbitrary in-plane direction can be analyzed. A substantial difference between the spin relaxation times can be expected for spins oriented along the in-plane directions [110] and $[\bar{1}10]$.

We propose that such a system can be used as a “spin storage”: The rotation of spins from the z direction into the $[\bar{1}10]$ direction effectively stores the spins because the relaxation time for the latter direction is larger by orders of magnitude.

V. CONCLUSION

Starting from a realistic model for the anisotropic spin splitting in $\text{GaAs}/\text{AlGaAs}$ and $\text{InAs}/\text{AlGaSb}$ quantum structures we calculate the parameters which determine the longitudinal (τ_z^{-1}) and transverse (τ_{\pm}^{-1}) spin-relaxation rates and determine their dependence on QW width and carrier concentration. We quantify the previously predicted¹⁷ giant anisotropy of spin relaxation by our more realistic calculation of the spin splitting. In contrast with previous investigations our accurate calculations predict a pronounced nonmonotonic behavior of $\tau_-^{-1}(n)$, which can be understood by ascribing the spin relaxation to the transverse components of the effective magnetic field. Future work will include calculations for different material systems, growth directions and doping profiles. For comparison with room-temperature experiments the temperature dependence and the effects of different scattering mechanisms have to be considered. Furthermore, the microscopic interface asymmetry, that

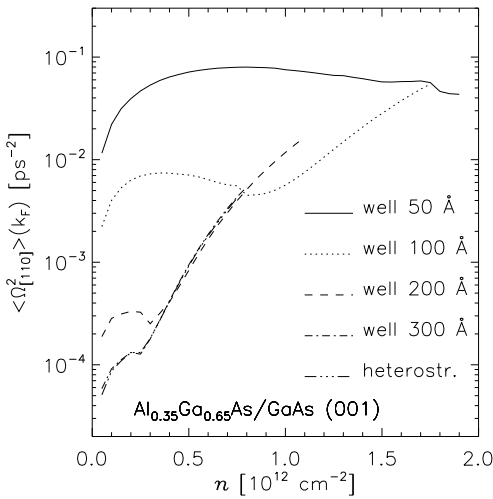


FIG. 7: Mean squared transverse field $\langle \Omega_{[110]}^2 \rangle(k_F)$ as a function of n for the AlGaAs/GaAs systems of Fig. 6.

has been identified as an additional mechanism of spin splitting,²⁹ will be taken into account.

Acknowledgments

We would like to thank L. E. Golub for valuable discussions. This work has been supported by the DFG via Forschergruppe 370 *Ferromagnet-Halbleiter-Nanostrukturen*.

* Electronic address: josef.kainz@physik.uni-regensburg.de

¹ D. P. DiVincenzo, Science **270**, 255 (1995).

² G. A. Prinz, Science **282**, 1660 (1998).

³ J. M. Kikkawa and D. D. Awschalom, Phys. Rev. Lett. **80**, 4313 (1998).

⁴ J. M. Kikkawa and D. D. Awschalom, Nature **397**, 139 (1999).

⁵ J. M. Kikkawa, I. P. Smorchkova, N. Samarth, and D. D. Awschalom, Science **277**, 1284 (1997).

⁶ A. Tackeuchi, Y. Nishikawa, and O. Wada, Appl. Phys. Lett. **68**, 797 (1996).

⁷ R. Terauchi, Y. Ohno, T. Adachi, A. Sato, F. Matsukura, A. Tackeuchi, and H. Ohno, Jpn. J. Appl. Phys. **38**, 2549 (1999).

⁸ A. Malinowski, R. S. Britton, T. Grevatt, R. T. Harley, D. A. Ritchie, and M. Y. Simmons, Phys. Rev. B **62**, 13034 (2000).

⁹ T. Adachi, Y. Ohno, F. Matsukura, and H. Ohno, Physica E **10**, 36 (2001).

¹⁰ G. E. Pikus and A. N. Titkov, in *Optical Orientation*, edited by F. Meier and B. P. Zakharchenya (Elsevier, Amsterdam, 1984).

¹¹ M. I. D'yakonov and V. I. Perel', Sov. Phys. JETP **33**, 1053 (1971).

¹² M. I. D'yakonov and V. I. Perel', Sov. Phys. Solid State **13**, 3023 (1972).

¹³ G. L. Bir, A. G. Aronov, and G. E. Pikus, Sov. Phys. JETP **42**, 705 (1976).

¹⁴ N. S. Averkiev, L. E. Golub, and M. Willander, Semicond. **36**, 91 (2002).

¹⁵ G. Dresselhaus, Phys. Rev. **100**, 580 (1955).

¹⁶ Y. A. Bychkov and É. I. Rashba, JETP Lett. **39**, 78 (1984).

¹⁷ N. S. Averkiev and L. E. Golub, Phys. Rev. B **60**, 15582 (1999).

¹⁸ R. Winkler and U. Rössler, Phys. Rev. B **48**, 8918 (1993).

¹⁹ M. Braun and U. Rössler, J. Phys. C: Solid State Phys. **18**, 3365 (1985).

²⁰ M. I. Dyakonov and V. Y. Kachorovskii, Sov. Phys. Semicond. **20**, 110 (1986).

²¹ F. F. Fang and W. E. Howard, Phys. Rev. Lett. **16**, 797 (1966).

²² A. R. Hamilton, E. H. Linfield, M. J. Kelly, D. A. Ritchie, G. A. C. Jones, and M. Pepper, Phys. Rev. B **51**, 17600 (1995).

²³ L. Wissinger, U. Rössler, R. Winkler, B. Jusserand, and D. Richards, Phys. Rev. B **58**, 15375 (1998).

²⁴ U. Rössler, Solid State Commun. **49**, 943 (1984).

²⁵ W. H. Lau, J. T. Olesberg, and M. E. Flatté, Phys. Rev. B **64**, 161301(R) (2001).

²⁶ C. P. Slichter, *Principles of Magnetic Resonance* (Harper & Row, New York, 1963).

²⁷ S. Datta and B. Das, Appl. Phys. Lett. **56**, 665 (1990).

²⁸ J. A. Gupta, R. Knobel, N. Samarth, and D. D. Awschalom, Science **292**, 2458 (2001).

²⁹ U. Rössler and J. Kainz, Solid State Commun. **121**, 313 (2002).

³⁰ H. Mayer and U. Rössler, Phys. Rev. B **44**, 9048 (1991).

³¹ The difference between the value of $\gamma = 27 \text{ eV}\text{\AA}$ from Ref. 14 and our value is due to taking into account the coupling parameter Δ^- (see Ref. 30).

³² We choose our coordinate system such that the electric field points in [001] direction, whereas in Ref. 14 the electric field points in the opposite direction, which leads to an interchange of τ_+ and τ_- .